MOLECULAR AND CELLULAR BIOLOGY, Oct. 1993, p. 6558–6571
0270-7306/93/106558-14$02.00/0

Vol. 13, No. 10

A Family of Human Phosphodiesterases Homologous to the *dunce* Learning and Memory Gene Product of *Drosophila melanogaster* Are Potential Targets for Antidepressant Drugs

GRAEME BOLGER,[1] TAMAR MICHAELI,[1]† TIM MARTINS,[2] TOM ST. JOHN,[2] BART STEINER,[2] LINDA RODGERS,[1] MICHAEL RIGGS,[1] MICHAEL WIGLER,[1]* AND KENNETH FERGUSON[2]

Cold Spring Harbor Laboratory, P.O. Box 100, Cold Spring Harbor, New York 11724,[1] and ICOS Corporation, Bothell, Washington 98021[2]

Received 28 April 1993/Returned for modification 1 July 1993/Accepted 26 July 1993

We have isolated cDNAs for four human genes (DPDE1 through DPDE4) closely related to the *dnc* learning and memory locus of *Drosophila melanogaster*. The deduced amino acid sequences of the *Drosophila* and human proteins have considerable homology, extending beyond the putative catalytic region to include two novel, highly conserved, upstream conserved regions (UCR1 and UCR2). The upstream conserved regions are located in the amino-terminal regions of the proteins and appear to be unique to these genes. Polymerase chain reaction analysis suggested that these genes encoded the only homologs of *dnc* in the human genome. Three of the four genes were expressed in *Saccharomyces cerevisiae* and shown to encode cyclic AMP-specific phosphodiesterases. The products of the expressed genes displayed the pattern of sensitivity to inhibitors expected for members of the type IV, cyclic AMP-specific class of phosphodiesterases. Each of the four genes demonstrated a distinctive pattern of expression in RNA from human cell lines.

Regulation of cyclic AMP (cAMP) is important in central nervous system (CNS) function in both invertebrates and mammals. Studies of two different invertebrates in particular have demonstrated a role for cAMP in learning and memory. In *Aplysia* snails, long-term facilitation of neurons in the gill retraction reflex occurs with learning. These neuronal changes are associated with alterations in activity of several components of the cAMP signalling pathway, particularly adenylyl cyclase and a cAMP-dependent protein kinase (32). In *Drosophila melanogaster*, numerous mutations in genes affecting learning have been isolated, including *dunce* (*dnc*), which encodes a cAMP-specific phosphodiesterase (PDE), and *rutabaga* (*rut*), which encodes a calcium-calmodulin-stimulated adenylyl cyclase (10, 16, 28). Electrophysiologic studies of neurons from *dnc*$^-$ and *rut*$^-$ flies have shown alterations in synaptic plasticity, suggesting that the functional changes occurring in learning in wild-type flies are similar to those seen in *Aplysia* snails (40). These observations suggest that modulation of the cAMP pathway can influence learning and memory in organisms widely separated in evolution.

Evidence for a functional role of dunce-like PDEs in the mammalian CNS initially came from the development of specific inhibitors. Inhibitors of cAMP-specific PDEs, including the drug rolipram, have clinical activity as antidepressants (11). The initial biochemical analysis of mammalian CNS PDEs, and of these inhibitors, was limited to testing in partially purified preparations, which can contain multiple PDE isoforms (1). More recently, cDNAs for homologs of *dnc* have been cloned from rats (5, 7, 9, 36–38) and shown to be rolipram sensitive (14, 37, 38). One of these homologs, DPD, was cloned by us in the course of developing genetic screens for mammalian genes that interact with the RAS-cAMP pathway in the yeast *Saccharomyces cerevisiae*. Although the rat *dnc* homologs are encoded by at least four different genes, only two cDNAs encoding a *dnc* homolog have been isolated from humans (17, 24). In this report, we demonstrate that four human *dnc*-related loci exist and that the diversity of dunce-related gene products is further augmented by isoforms generated by alternative splicing. We also provide evidence that our human homologs are targets for antidepressant drugs.

MATERIALS AND METHODS

All procedures not detailed below were performed as described by Sambrook et al. (31). Procedures involving *S. cerevisiae* were performed as described by Rose et al. (29).

Degenerate primer PCR. Polymerase chain reactions (PCRs) (30) were initially performed with DNA isolated from cDNA libraries as a template. To reduce background in the PCRs from the λZAP vector arms, the plasmid pBluescript, containing the cDNA insert, was excised in vivo, with a mass scale-up of the procedure previously described (34). A total of 200 ng of this DNA was used in PCRs, with *Taq* polymerase (30). PCR conditions consisted of 40 cycles of 94°C for 1 min 30 s, 55°C for 3 min, and 72°C for 5 min. The oligonucleotide primers used in these reactions (pairs HDUN3 and HDUN5, HDUN4 and HDUN11, and HDUN4 and HDUN6, respectively [Table 1]) represented the degenerate coding sequence (or its complement) of regions conserved between the rat DPD gene and *dnc* (Fig. 1 and 2).

PCR was also performed on first-strand cDNA, which was synthesized from polyadenylated RNA isolated from human temporal cortex (obtained from patients undergoing surgery for epilepsy, but grossly normal in appearance). RNA was isolated by the guanidine thiocyanate-cesium chloride method (20), and first-strand cDNA was prepared with oligo(dT) priming and avian myeloblastosis virus reverse transcriptase (31). Approximately 200 ng of cDNA was used in PCRs as described above. PCR was also performed on genomic DNA, with either 10 ng of DNA from genomic

* Corresponding author.
† Present address: Department of Developmental Biology and Cancer, Albert Einstein College of Medicine, Bronx, NY 10461.

TABLE 1. PCR primers used in this study[a]

Name	Sequence, 5′ to 3′	Translation	Location[b]
HDUN3	GAGGTACCACYTTYTTNGTYTCNACCAT	MVETKKV[c]	459
HDUN4	CTAGCAGTGCGGTACCGCCCANGTYTCCCANARNGG	PLWETWA[c]	552
HDUN5	GAATTCATHCAYGTNGAYCAYCC	IHDVDHP	372
HDUN6	CGATGCTACGGAATTCGAYATGWSNAARCAYATG	DMSKHM	445
HDUN11	CGATGCTACGGAATTCAARATGGTNATHGAYATNGT	KMVID(I/M)V	435
HDUN20	CTAGCAGTGCGTTACCACNATRTCDATNACCATYTT	KMVID(I/M)V[c]	435
HDUN24	CGATGCTACGGAATTCTTYAARYTNYTNCARGRNGA	FKLLQ(E/A)E	411

[a] The abbreviations for positions containing degeneracies are as follows: H = A or C or T; N = A or C or G or T; R = A or G; S = C or G; W = A or T; Y = C or T.
[b] Location on the *dnc* sequence (Fig. 2A).
[c] Primes off the noncoding strand.

clones (see below) or 200 ng of human placental DNA, in reactions otherwise identical to those described above.

To analyze the PCR products, the reaction was purified by agarose gel electrophoresis and the DNA was cleaved at the restriction sites in the PCR primers and cloned into pUC119 (31). The inserts of approximately 80 recombinant clones from each PCR were then individually sequenced. For this purpose, single-strand template was prepared by PCRs as described above, but with primers recognizing sequences on the pUC119 plasmid, added to the PCR in a 1:0.005 molar ratio. The primers had the following sequences (5′ to 3′): AACAGCTATGACCATGATTA and AGGGTTTTCCCAG TCACGAC. This template was then used in sequencing reactions with Sequenase, in a modification of the procedures outlined by the manufacturer (United States Biochemical, Cleveland, Ohio). The changes from the standard protocol were as follows: (i) as a sequencing primer, an oligomer (M13-20 primer; New England Biolabs) was labelled with ^{32}P by using kinase; (ii) the ^{35}S-dATP and the initial elongation step were both omitted; and (iii) manganese was used in all reactions.

Hybridization screening of cDNA and genomic libraries. Initial screening used the complete insert from the rat DPD cDNA clone (5) at low stringency (hybridization, 6× SSC [1× SSC is 0.15 M NaCl plus 0.015 M sodium citrate]–0.5% sodium dodecyl sulfate [SDS], 50°C; final wash, 0.1× SSC–0.1% SDS, 50°C), to screen a human temporal cortical cDNA library. Incomplete cDNA clones from three different loci (DPDEs 2, 3, and 4) were isolated, and these were subsequently used to screen other libraries in an attempt to obtain longer ones. These libraries contained cDNA derived from human fetal brain (the source of pPDEs 39, 43, and 46), human frontal cortex (pPDE32), or human temporal cortex (pPDE21), cloned into the *Eco*RI site of λZAP (Stratagene, La Jolla, Calif.). They were screened at high stringency (as above, but with a final wash of 0.1× SSC–0.1% SDS at 68°C). Genomic clones were isolated from a human placental DNA library cloned into λFIX II (Stratagene). pTM72, pPDE46, pPDE43 (or clones corresponding to various regions thereof) and the complete insert of pPDE21 were used as probes. Screening was performed at high stringency (final wash, 0.1× SSC–0.1% SDS, 68 to 70°C).

Northern (RNA) blotting and RNase protection analysis. For Northern blotting, polyadenylated RNA from human temporal cortex (see above) was electrophoresed through formaldehyde-agarose, transferred to nitrocellulose (31), and hybridized to [^{32}P]dCTP-labelled probes generated by random priming. The probe for pTM72 corresponded to nucleotides (nt) 2422 to 3181. For pPDE46, pPDE43, and pPDE21, the probes corresponded to the sequence from codons 693 of pPDE46, 611 of pPDE43, and 222 of pPDE21, respectively (Fig. 2A), to the 3′ noncoding regions of these clones (nt 2733 for pPDE46, 2788 for pPDE43, and 1155 for pPDE21). Washing was at high stringency (final wash, 0.1× SSC–0.5% SDS, 68°C), and exposure was for 7 days at −70°C, with intensifying screens.

For RNase protection analysis, total RNA was isolated from human tumor cell lines (20). All the cell lines used are available from the American Type Culture Collection (Rockville, Md.). Total RNA was also similarly isolated from testes removed from patients undergoing therapy for carcinoma of the prostate. Single-stranded antisense RNA probes were generated from appropriate regions of the four cDNAs, cloned under the control of the SP6 promoter (in pGEM3Zf or pGEM4Zf [Promega, Madison, Wis.]). The probes were designed to hybridize to the regions of the mRNAs encoding the divergent carboxyl termini of the dunce proteins. For pPDE46, the probe corresponded to the sequence from codons 693 to 768 (Fig. 2A). For the other cDNAs, the probes were located in noncoding DNA 3′ to the termination codon, i.e., for pTM72, nt 2828 to 3181; for pPDE43, nt 2628 to 2788; and for pPDE21, nt 786 to 1155. RNase protection assays were performed as described previously (31). RNase digestion was done with 20 μg of RNA per assay and RNases A and T_1 (Worthington) for 1 h at 30°C. Autoradiograms of the gels were exposed for 5 days at −70°C.

Construction of clones for biochemical and pharmacological assays. Fragments of pTM72, pPDE46, pPDE43, and the *dnc* type II cDNA were cloned into the *Not*I site of pADANS (6). All the resulting constructs produced a transcript generated off the *S. cerevisiae* alcohol dehydrogenase promoter and contained 13 amino acids at their amino termini derived from the alcohol dehydrogenase gene product, in frame with the open reading frame (ORF) of the human cDNA. These constructs were designed to provide an initiation sequence known to function in *S. cerevisiae*. The inserts were generated by PCR, with *Pfu* polymerase, as described previously (19). PCRs were performed with 20 cycles of 94°C for 1 min 30 s, 65°C for 2 min, and 72°C for 5 min. *Not*I sites were incorporated into the PCR primers to aid in subsequent cloning.

PDE activity assay. Cells used in biochemical and pharmacologic studies were isolated at mid-log phase of growth at 30°C on selective medium (SC-leucine). Pellets containing approximately 10^{10} cells (1 g [wet weight]) were resuspended in 20 mM Tris-HCl (pH 8.0)–5 mM EDTA–5 mM EGTA [ethylene glycol-bis(β-aminoethyl ether)-*N*,*N*,*N*′,*N*′-tetraacetic acid]–1 mM *o*-phenanthroline–0.1 mM 4-(2-aminoethyl)-benzenesulfonylfluoride–1 mM benzamidine–10 μg of leupeptin per ml–10 μg of pepstatin per ml–10 μg of aprotinin

per ml–10 μg of both calpain inhibitors I and II per ml. Cells were lysed by rapid mixing with glass beads and centrifuged at 10,000 × *g* for 10 min to remove cell debris. Aliquots of the supernatant were assayed for PDE activity immediately or stored at −80°C for later analysis. Protein was measured by the method of Bradford (3) with a kit (Pierce, Rockford, Ill.).

Cyclic nucleotide PDE activity was assayed as previously described, with modifications (22, 25). Assays were performed in vinyl microtiter plates at 30°C. Incubation mixtures contained 40 mM Tris-Cl (pH 8.0), 1 mM EGTA, 5 mM magnesium chloride, 0.1 mg of bovine serum albumin per ml, diluted enzyme, [^{3}H]cAMP (1.3 to 7.5 μCi/ml; NEN Inc., Boston, Mass.), [^{14}C]AMP (0.11 μCi/ml; NEN Inc.), and various amounts of unlabelled cyclic nucleotides in a total volume of 100 μl. Assays were performed for 15 min. Three minutes prior to termination of the reaction, 5 μl of *Crotalus atrox* snake venom 5′ nucleotidase (Sigma, St. Louis, Mo.; 15 mg/ml) was added. The assays were terminated by adding 50 μl of 20 mM Tris-Cl (pH 7.5)–100 mM EDTA–0.15% cetylpyridinium chloride. The nucleoside products were separated from the unreacted cyclic nucleotides by anion-exchange chromatography on Sephadex A-25 (Pharmacia, Piscataway, N.J.) columns (8 by 30 mm). After sample application, the columns were washed with 0.25 ml of 25 mM Tris-Cl, pH 7.5, and then eluted with three applications (0.5 ml) of the same buffer. The eluate was mixed with EcoLume (ICN Biochemicals, Irvine, Calif.) and analyzed for ^{3}H and ^{14}C content by dual-channel liquid scintillation spectroscopy. The recovery of ^{3}H nucleotide reaction products were corrected for the recovery of [^{14}C] AMP.

For estimation of kinetic parameters, the PDE assays utilized a constant radioisotopic specific activity of 0.03 μCi/nmol of [^{3}H]cAMP. Initial rates of hydrolysis were determined from five duplicate fourfold dilutions of the initial extract stock, with cAMP concentrations ranging from 0.1 to 300 μM. Only those enzyme dilutions that yielded less than 30% hydrolysis of the total substrate in 15 min were included in the final rate determination. The kinetic data were fit to a Michaelis-Menten model with TableCurve (Jandel Scientific, San Rafael, Calif.) to obtain estimates of the apparent K_m, V_{max} (enzymatic specific activity), and associated errors. The model used the equation $y = (ax)/(b + x)$, where y is velocity, x is [cAMP], a is V_{max}, and b is K_m.

Inhibitor analysis was performed with 1 μM cAMP as the substrate. Milrinone and IBMX were from Sigma; rolipram was from BIOMOL Research Laboratories (Plymouth Meeting, Pa.); 8-methoxy-IBMX was a kind gift from Jack Wells, Vanderbilt University; and zaprinast was a kind gift from Paul Feldman, Glaxo Inc. Research Institute (Research Triangle Park, N.C.). Denbufylline and cilostamide (OPC 3689) were synthesized by published procedures (13, 18). Inhibitory compound stocks were initially made up in 100% dimethyl sulfoxide (Aldrich), and final dimethyl sulfoxide concentrations in the PDE assay never exceeded 1% (vol/vol). Data were normalized to protein concentration and represent estimates of initial rates, determined by incubations at multiple enzyme dilutions.

Dose-response inhibitory curves were fitted with a four-parameter logistic dose-response model described by the equation $y = a + b/[1 + (x/c)^d]$, where y is percent total PDE activity, a is the minimum activity level, b is the maximal activity level, c is the inhibitor concentration at 50% maximal activity (IC_{50}), x is the inhibitor concentration, and d is a parameter that determines the slope of the curve at the IC_{50}. The four-parameter model was used for fitting the inhibitor data because the inhibitory curves frequently spanned a broader range of inhibitor concentrations than would be fit accurately by a simpler model. The ability to adjust the slope inherent in the four-parameter logistic curve permitted a better fit to these data. However, for certain data sets, a two-parameter model was used to provide an estimate of the IC_{50}; it is described by the equation $y = b/[1 + (x/c)]$, where y is percent total PDE activity, b is the maximal activity level, c is the IC_{50}, and x is the inhibitor concentration. This model assumes a baseline of zero activity and does not permit variation in the slope at the IC_{50}. It was used for two categories of data sets: (i) when activity could not be reduced to baseline, even at high inhibitor concentrations (i.e., IC_{50} greater than 500 μM), or (ii) when data sets were too variable to estimate the baseline.

Nucleotide sequence accession numbers. The sequences in this paper have been communicated to the GenBank/EMBL data bases under the following accession numbers: L20965, L20966, L20967, L20968, L20969, L20970, and L20971. The human locus names in this paper have been communicated to the Human Genome Nomenclature Committee.

RESULTS

Cloning of human dunce-like PDEs. The initial objective of this study was to clone cDNAs for all homologs of *dnc* in the human genome. For this purpose, three independent methods were utilized. The first approach used PCR to amplify human cDNA with homology to sequences present in both *dnc* and rat DPD. This approach was used to analyze cDNA from several regions of human brain, and four different sequences, each highly homologous to *dnc*, were obtained. The second approach used low-stringency hybridization, with the DPD cDNA as a probe, to probe cDNA libraries from human brain. This approach yielded cDNA clones which collectively contained the same four sequences obtained by PCR. These cDNA clones are described in more detail below. The third approach was to isolate cDNAs that could suppress the heat shock-sensitive phenotype of strains of *S. cerevisiae* with mutations in the RAS-cAMP pathway. Activating mutations of this pathway produce at least a portion of their phenotype by raising intracellular cAMP levels, and introduction of an exogenous PDE into these cells can lower cAMP levels sufficiently to restore heat shock resistance. Two different screens, both previously reported (6, 25), were performed on a cDNA library from a human glioblastoma cell line. One of these screens isolated suppressors of the *S. cerevisiae RAS2*$^{Val\text{-}19}$ mutation, while the other yielded supressors of an *S. cerevisiae* strain (10DAB) with disruptions of both endogenous *PDE* genes. Both these screens generated cDNAs encoded by several different human genes. Only some of these clones were homologous to *dnc*, and only these are described here.

These three approaches demonstrated that four different human loci, which we call DPDE1, DPDE2, DPDE3, and DPDE4, encode cDNAs strongly homologous to that of *dnc*. The longest and most complete of the cDNAs from each of these loci are presented in Fig. 1. The clones pPDE21, pPDE32, pPDE39, pPDE43, and pPDE46 were all obtained from the low-stringency screen described above. The pTM3 and pTM72 clones were isolated from the *S. cerevisiae* genetic screens.

Putative alternative splicing and other variants of the DPDE2, -3, and -4 transcripts. Comparison of the sequences of different cDNAs from the DPDE2, -3, and -4 genes

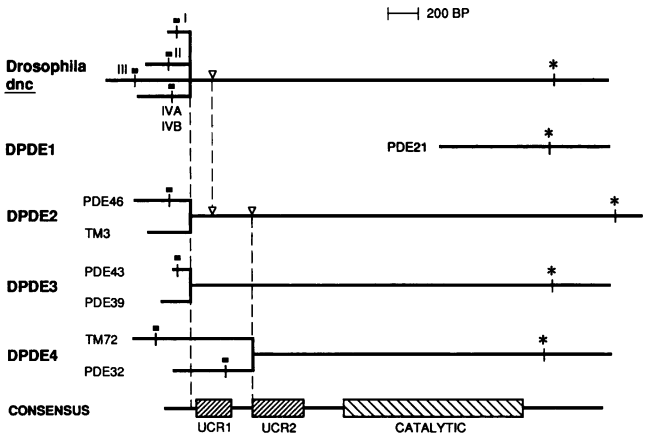

FIG. 1. cDNAs from the four human *dunce* loci, aligned with those from the *Drosophila dnc* locus. Regions of variant sequence in the clones from each locus are shown by branched lines. Areas of common sequence are shown by merged lines. Vertical dashed lines indicate homologous divergence points that occur in clones from different loci. The positions of putative initiation and termination codons are marked by small boxes and asterisks, respectively. Regions of strong sequence conservation are shown in the areas defined by hatched boxes. The UCR1 consensus is not found in pPDE32. Roman numerals indicate the various alternatively spliced isoforms from the *dnc* locus (28). The small inverted triangle above the *dnc* cDNA indicates the location of the alternatively spliced exon 4 seen in some of these isoforms (types I, II, and IVA). Exon 3 of *dnc* is found between these two points of alternative splicing. The small inverted triangles above the DPDE2 cDNAs indicate the positions of the insertions in pTM3.

revealed that each locus produced clones with regions of variant sequence (Fig. 1). The most common variations were seen in the DPDE2 and DPDE3 loci and consisted of substitutions of blocks of sequences 5′ to the phenylalanine codon which marks the start of homology between the human and *Drosophila* cDNA clones (Fig. 1 and 2). This location is homologous to the beginning of *dnc* exon 3, where considerable alternative splicing occurs (28).

Two cDNA clones (pPDE32 and pTM72) from the DPDE4 locus also contained alternative coding sequences at their 5′ end (Fig. 1 and 2B). The point of divergence is not known to be an alternative splice site in *dnc*, but does correspond to one of the insertions in pTM3 (see below). The deduced amino acid sequences of the alternative amino-terminal regions showed no obvious homology to each other, but the sequences of both were strongly conserved (76 and 74% exact amino acid homology, respectively) for alternative transcripts from the corresponding locus in rats (2).

Finally, one clone, pTM3, contained two insertions of blocks of sequence, which disrupt its ORF. These blocks are not seen in pPDE46 or in any other cDNA clone we have isolated from this locus and have no sequence homology to any human or *Drosophila* gene. Splice consensus sequences are apparent at three of the four ends of these blocks. We believe that these blocks are improperly spliced introns and that pTM3 encodes a protein that is unlikely to be normally found in human cells but can function genetically in *S. cerevisiae* (possibly by initiating translation 3′ to the insertions). The insertions occur at points of alternative splicing in the *dnc* or human loci (Fig. 1), suggesting that at least some of the genomic structure of the *dunce* genes is conserved in evolution.

Further analysis of mRNA and genomic DNA is needed to confirm that our variant clones are alternatively spliced isoforms, as opposed to unprocessed RNA transcripts, or processing intermediates. However, it is unlikely that they arose as artifacts of ligation, as each of the variants (except the insertions in pTM3) was seen in at least two different cDNA clones. Additional mRNA variants from these loci may also exist.

The alignment of *Drosophila* and human dunces. Sequence analysis of the seven human *dunce*-like cDNA clones in Fig. 1 showed that four of them (pPDE46, pPDE43, pPDE32, and pTM72) contain complete ORFs, with stop codons in all three reading frames upstream of the putative initiation ATG. The ORF of pPDE39 is open at its 5′ end, and a possible initiation ATG is shown in Fig. 2A, although the ORF may continue amino terminal to this point. pPDE39 also ends at amino acid 419 of pPDE43, before the termination codon of DPDE3 transcripts is reached. The ORF of pPDE21 is open at its 5′ end but continues to its putative termination codon. pTM3 contains a single ORF that is disrupted by the insertions (see above), as well as by several single-nucleotide deviations from the corresponding sequence of pPDE46, which may represent sequence ambiguities or polymorphisms. The termination codons of *dnc* and the cDNAs for the DPDE1, DPDE3, and DPDE4 loci are all within 20 codons of each other (Fig. 1 and 2A), whereas that of pPDE46 is located about 100 codons 3′ to this region. The sequence of pPDE46 3′ to this region is identical to that of pTM3 and other clones we have isolated for this locus.

The alignment of the deduced amino acid sequences of these clones showed impressive homology to *dnc* (Fig. 2A and 3). Alternative mRNA splice variants of *dnc* that did not contain exon 4 required the fewest gaps for alignment (Fig. 1) (28). The homology begins at the phenylalanine corresponding to the beginning of *dnc* exon 3 and then becomes very striking in two regions of homology, neither of which has been previously recognized, that we call upstream conserved regions (UCR1 and UCR2). UCR1 and UCR2 are separated from each other, and from the catalytic region closer to the carboxyl terminus, by regions of lower homology in which there is also heterogeneity in length. The beginning of UCR2 also corresponds to the point of putative alternative splicing in the DPDE4 locus (i.e., pTM72 contains UCR1 but pPDE32 does not). In contrast, the N-terminal alternate regions of the genes were strongly divergent. Neither *Drosophila* nor human sequences showed any homology in these regions, with the exception of a single block of conserved amino acids (12 of 15 identical) in the pPDE46 and pPDE39 clones (Fig. 2B).

Comparison of the dunce PDE sequences to those of other families of cyclic nucleotide PDEs shows both conserved and novel features. The dunce catalytic region has weak, but significant, homology (approximately 30% amino acid identity) to the catalytic regions of other PDE classes (1, 9, 25, 36). The UCR1 and UCR2 regions, however, have no apparent homology to the sequence of any non-dunce PDE, or with those of any other genes in the EMBL, GenBank, and Swiss Protein data bases. The strong evolutionary conservation of the UCR1 and UCR2 regions among the dunce PDEs suggests that they are important in dunce PDE function (see Discussion).

Livi et al. have isolated a dunce-like PDE cDNA from a human blood monocyte line which corresponds to our pPDE46 but is truncated at its amino terminus (17). However, this truncated cDNA includes the complete catalytic region and encodes a biochemically active, rolipram-inhib-

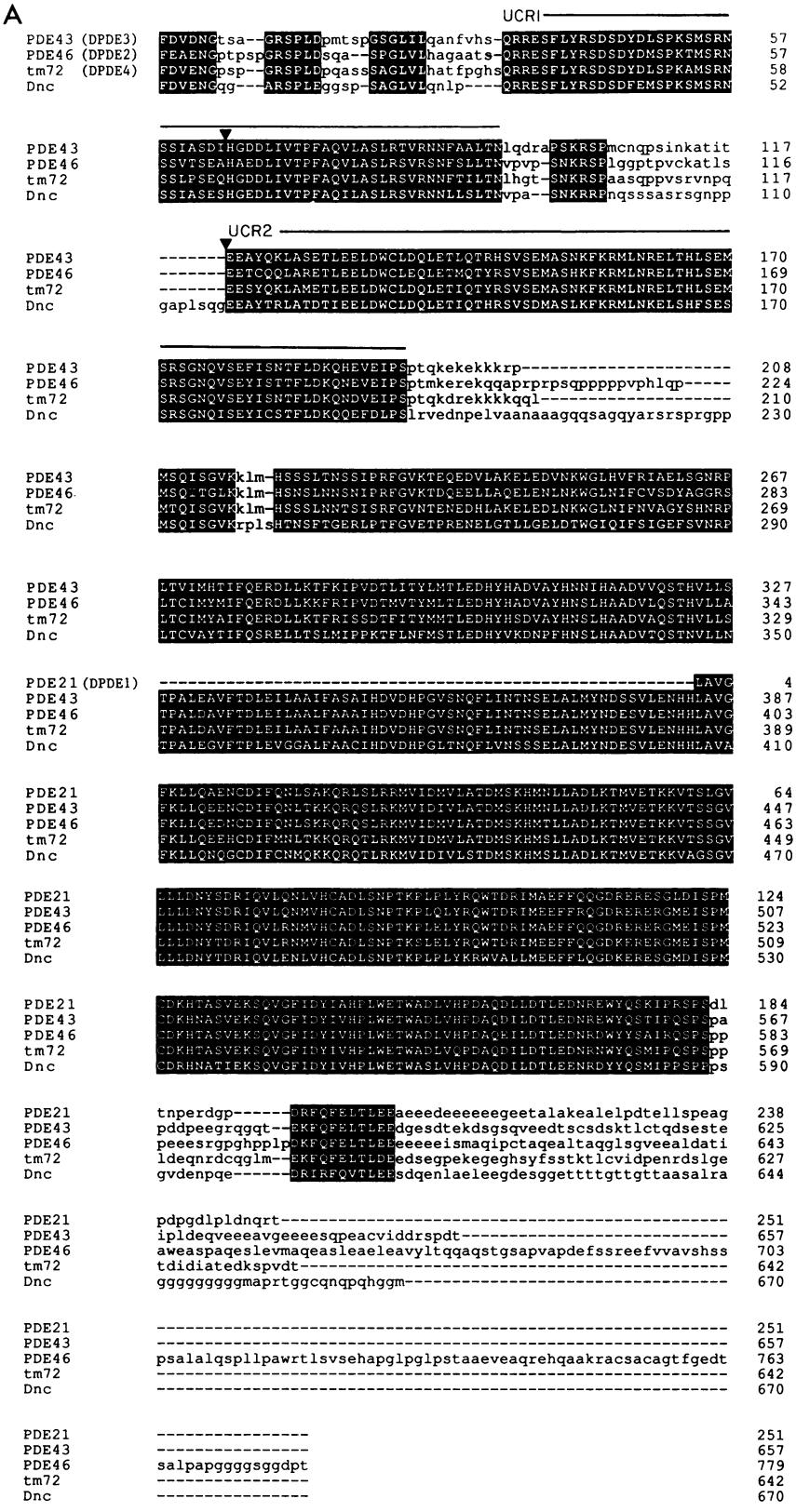
A
UCR1
PDE43 (DPDE3)
PDE46 (DPDE2)
tm72 (DPDE4)
Dnc
UCR2
PDE21 (DPDE1)

B

```
TM3    1                    glgripelqlvafpvavaaedeaflpeplapr
      33 aprrprsppsspvffaspsptfrrrlrllrscqdlgrqawagagfeaeng--

PDE46  1                                          mepptvpsersls
      14 lslpgpregqatlkpppqhlwrqprtpiriqqrgysdsaeraererqphr
      64 pieradamdTsdRPGLrttRMSWPSSFhGtgtgsggagggssrrfeaeng--
                 |  ||||: :||||||||  |
PDE39  1 mdrtsyaveTghRPGLkksRMSWPSSFqG.............lrrfdvdng--

PDE43  1                                  mmhvnnfpfrrhswicfdvdng--

 TM72  1 mkksrsvmtvmaddnvkdyfecslsksysssntlgidlwrgrrccsgnl
      50 qlpplsqrqserartpegdgisrpttlplttlpsiaittvsqecfdveng--

PDE32  1       mkehggtfsstgisggsgdsamdslqplqpnymvpvclfaeesvqk--
```

FIG. 2. Deduced amino acid sequences of the cDNAs of the four human *dunce* genes. The nucleotide sequences are available from GenBank. (A) Alignment of the homologous portions of pTM72, pPDE46, pPDE43, and the type IVB splicing product of *dnc* (exons 3 to 13, excluding exon 4 [28]). The available sequence from pPDE21 is also shown. Alignments were performed with the MACAW program (33). The two upstream conserved regions, UCR1 and UCR2, are delineated with heavy horizontal lines. The small triangles above the alignments indicate the positions of the insertions in pTM3. (B) The deduced amino acid sequences of the amino-terminal regions of the cDNA clones. Sequence that overlaps with the alignment in panel A is underlined. Capital letters and vertical lines (or colons) show the area of sequence conservation between pPDE39 and pPDE46. Dots and dashes indicate gaps which facilitate these alignments. Note that the sequence of pPDE39 may continue aminoterminal to the methionine shown here (see Results).

ited PDE. The DNA sequence of their clone also contains a number of single-nucleotide changes which alter their ORF 5′ from the proline at position 103 of pPDE46 (Fig. 2A). We believe that the deduced amino acid sequence upstream from this point of pPDE46 is correct, because it is conserved in the homologous regions of the *Drosophila*, DPDE3, and DPDE4 genes. The data of Livi et al. may reflect sequencing or cloning errors in this region, although the presence of polymorphisms cannot be rigorously excluded. More recently, McLaughlin et al. have isolated a clone whose deduced amino acid sequence is identical to that of our pPDE32 (24).

Enumeration of the human genes. To search for additional *dnc* homologs in the human genome, the PCR approach used initially in this study for cDNA was extended to genomic DNA. Genomic DNA was studied because not necessarily all dunce-like PDE loci could be expressed in the cDNA libraries that were studied previously. We prepared PCR primers corresponding to the fully degenerate codons of nine different regions of amino acids that were conserved between the *Drosophila*, human, and rat *dunce* genes. Pairs of these primers (a total of 19 pairs) and either human genomic DNA, human *dunce* cDNA clones, or human *dunce* genomic clones were used in PCRs as described above. When genomic DNA was used as a template, the majority of these primer pairs each produced several PCR products. These were of different sizes, all larger than those produced by that pair with cDNA. When genomic clones were used as templates, they each produced single bands, identical in size to one of those seen with genomic DNA as a template. We therefore inferred that each of the bands with genomic DNA was produced from a different gene, by priming off sequences separated by an intron. The products were of different sizes because the lengths of these introns presumably varied among the *dunce* genes. However, two of the PCR primer pairs each produced a single band from genomic DNA, which was identical in size to those from the genomic clones and to that from cDNA. We concluded that these single bands were produced by priming off sequences located on a single exon. The PCR products produced from genomic DNA by one of these primer pairs (HDUN24 and HDUN20 [Fig. 2B; Table 1]) were cloned, and sequences from 79 individual clones were analyzed. Four different sequences were obtained: 9 from DPDE1, 29 from DPDE2, 25 from DPDE3, and 16 from DPDE4. No other PCR products homologous to *dnc* were found, and therefore, we

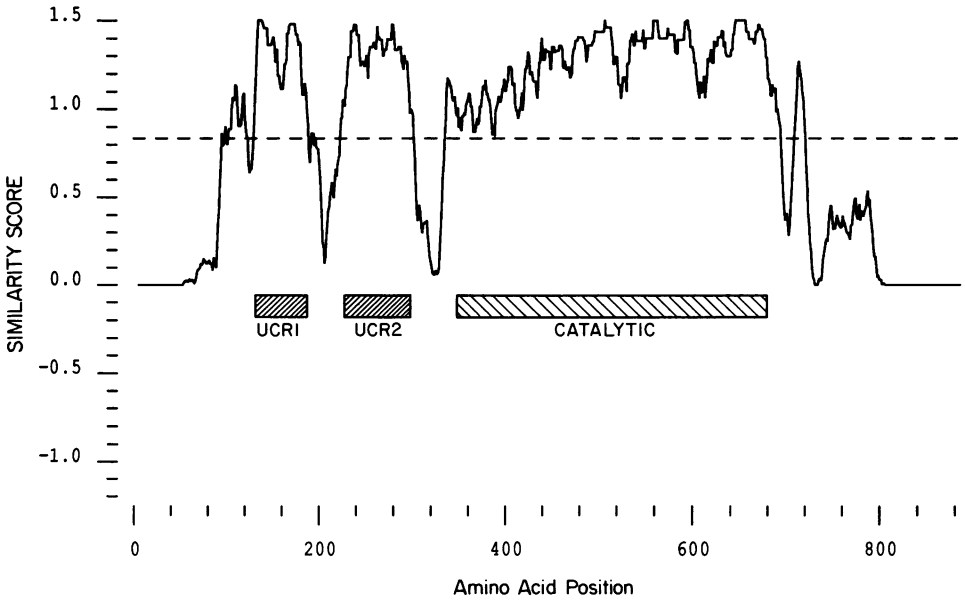

FIG. 3. Quantitative assessment of homology among the full-length cDNA clones for *dnc*, pPDE46, pPDE43, and pTM72, as measured by the PLOTSIMILARITY program (12). Bars indicate UCR1, UCR2, and the approximate location of the catalytic region, respectively. The horizontal dashed line indicates the margin of significance.

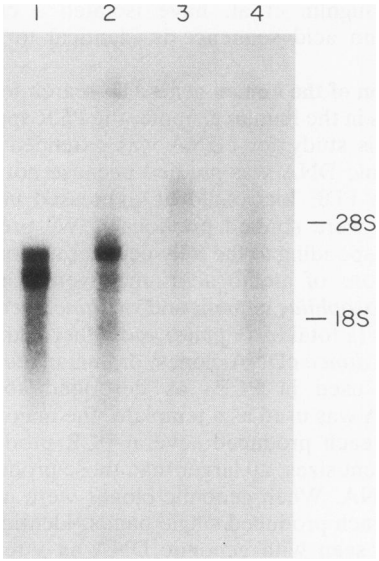

FIG. 4. Northern blotting of human brain polyadenylated RNA with probes from the human *dunce* cDNAs. Approximately 5 μg of RNA was applied per lane, each of which was individually hybridized to probes from the 3′ regions of one of the human dunce PDE cDNAs. Lanes 1 through 4 are with probes from pPDE46 (DPDE2 locus), pTM72 (DPDE4), pPDE43 (DPDE3), and pPDE21 (DPDE1), respectively.

conclude that there are likely to be only four *dnc* homologs in humans. We cannot totally exclude the existence of a homolog that, by chance, failed to anneal to these primers. Southern blotting and gene mapping have demonstrated that each human *dnc* homolog occurs as a single copy (26). We therefore attribute the differing abundances of the PCR products we obtained in this experiment to varying efficiency of PCR priming.

A total of four homologs of *dnc* have also been isolated from rats (5, 7, 9, 36, 37). We show elsewhere (2) that the rat genes have a 1:1 correspondence with their human counterparts. This pairwise relationship is apparent only upon comparison of coding sequences that lie outside the putative catalytic regions, not all of which are included among currently published rat *dunce* cDNA sequences. The human DPDE1 through DPDE4 loci each correspond, respectively, to the genes encoding ratPDE1 through ratPDE4 described by Swinnen et al. (36). Using the nomenclature of Beavo and Reifsnyder (1), our DPDE1 locus encodes the PDE isozyme IV_C, DPDE2 encodes isozyme IV_A, DPDE3 encodes isozyme IV_D, and DPDE4 encodes isozyme IV_B (see also Discussion).

Tissue distribution of the human *dunce* homologs. The expression and structure of the human *dunce*-like genes in the CNS was studied by Northern blotting. The probes in this study were specific to each of the four genes and recognized sequences 3′ to the consensus sequence QFELT LEE, which greatly differ among the four genes (Fig. 2B) (see Materials and Methods). With a probe for pTM72, bands of 4.6 and 4.0 kb in size were seen in polyadenylated RNA from surgically removed normal human temporal cortex. A band of 4.5 kb was seen with a pPDE46 probe, and the pPDE43 and pPDE21 probes produced no clearly detectable signal (Fig. 4). The 4.5-kb band detected by pPDE46 in brain tissue is similar to that observed by others in human tissues outside the CNS, with a similar probe (17). The two bands detected by pTM72 are also similar to those observed in a variety of human tissues by others using a similar probe (24). Since we obtained clones corresponding to pPDE43 and pPDE21 from a cDNA library derived from the same region of the human brain (temporal cortex) as the mRNA used in our Northern blots, we believe that these two genes also express transcripts in this region, although at very low levels.

The expression of the human homologs was also studied by RNase protection (Fig. 5). For this purpose, we prepared antisense RNA probes specific to each of the four genes, which, as in the Northern analysis, recognized sequences 3′ to the sequence QFELTLEE (see Materials and Methods). Analysis of total RNA from various cell lines with these probes demonstrated significant differences in expression among the four genes. Among the cell lines tested, transcripts from the DPDE1 locus appeared to be restricted to those of neuronal origin (the retinoblastoma line Y79 and the neuroblastoma line SK-N-SH). In contrast, transcripts from the DPDE2 locus were expressed in almost all the cell lines, although at different levels. Transcripts from the DPDE3 and DPDE4 loci were each present in distinctive patterns. Although these data are obtained from cell lines derived from tumors, they demonstrate that each of the DPDE loci can be expressed in a distinctive cell-specific pattern. In contrast to the data obtained by others with rats (36, 37), we saw little or no expression of the human *dunce* genes in the testis (lane 8, Fig. 5A to D). We believe that this reflects differences among these species, although the possibility of technical factors cannot be totally excluded.

Biochemical and pharmacologic properties of the *dunce* genes. To examine the biochemical and pharmacologic properties of the dunce PDEs, cDNA clones for *dnc* and three of the human genes (DPDEs 2, 3, and 4) were expressed in *S. cerevisiae* 10DAB, in which both endogenous PDE genes have been genetically disrupted (5). To ensure that any biochemical differences observed between the *dunce* genes reflected variations in their homologous coding regions, rather than potential differences in 5′ alternative splicing (see above), we prepared slightly truncated constructs of cDNAs from *dnc* (type II splice variant) and the three human loci, all of which started at the phenylalanine codon homologous to that at the beginning of *dnc* exon 3 (Fig. 1). Full-length constructs of the *dnc* type II and pTM72 cDNA clones were also analyzed. PDE assays were performed by a modification of previously described methods (22, 25). Because the pPDE21 clone encoded only a portion of the predicted protein, it was not tested in these assays.

The slightly truncated *dnc*, pTM72, pPDE46, and pPDE43 constructs all showed cAMP PDE activity (Fig. 6; Table 2). There was no detectable difference in biochemical activity between the truncated form of *dnc* and its full-length construct (Table 2). We have also observed no difference between the full-length pTM72 clone and its truncated construct (21). The K_m for cAMP for the three human clones ranged from 7×10^{-6} to 1.8×10^{-5} M, which was greater than that previously reported for mammalian cAMP-specific PDEs (0.5×10^{-6} to 4×10^{-6} M [7]). The K_m for cAMP for the full-length and truncated forms of *dnc* was approximately 3×10^{-5} M and about 3- to 15-fold higher than that previously reported for preparations of cAMP-specific PDE activity extracted from tissues of *D. melanogaster* (8, 14, 28).

We studied the effect of a number of PDE inhibitors on the activity of the human and *D. melanogaster* clones (Fig. 7; Table 3). The ability of these compounds to inhibit the

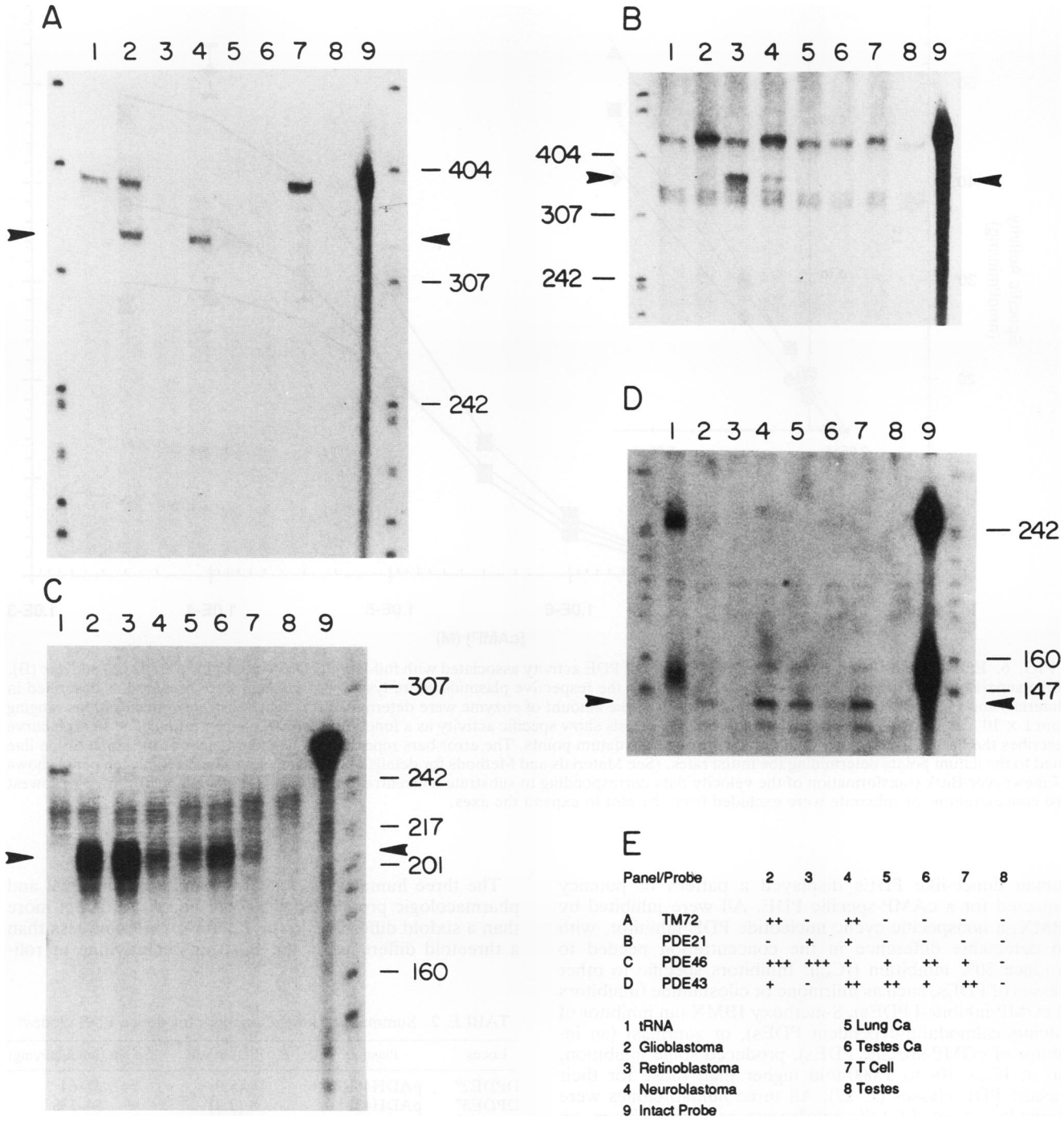

FIG. 5. RNase protection assays. Antisense RNA probes from the divergent 3′ regions of the cDNAs were used to probe RNA from various human tissues and cell lines. (A to D) Probes from pTM72 (DPDE4 locus), pPDE21 (DPDE1), pPDE46 (DPDE2), and pPDE43 (DPDE3), respectively. Lanes: 1, transfer RNA; 2, glioblastoma line U118; 3, retinoblastoma line Y79; 4, neuroblastoma line SK-N-SH; 5, lung small cell carcinoma line Calu 3; 6, testicular embryonal carcinoma line Cates 1B; 7, T-lymphoblast line Molt 3; 8, normal human testis; 9, probe without RNase. Size markers (base pairs) are *Msp*I-digested pBR322. The bands representing the protected RNA fragments are marked by the arrowheads. The predicted size of the pPDE43 probe was 160 nt, which corresponds to the smaller of the two bands seen on the gel. (E) Summary of the data in panels A through D. The signal produced by each RNA source, as determined visually from the autoradiograms, is presented relative to that of other samples with the same probe.

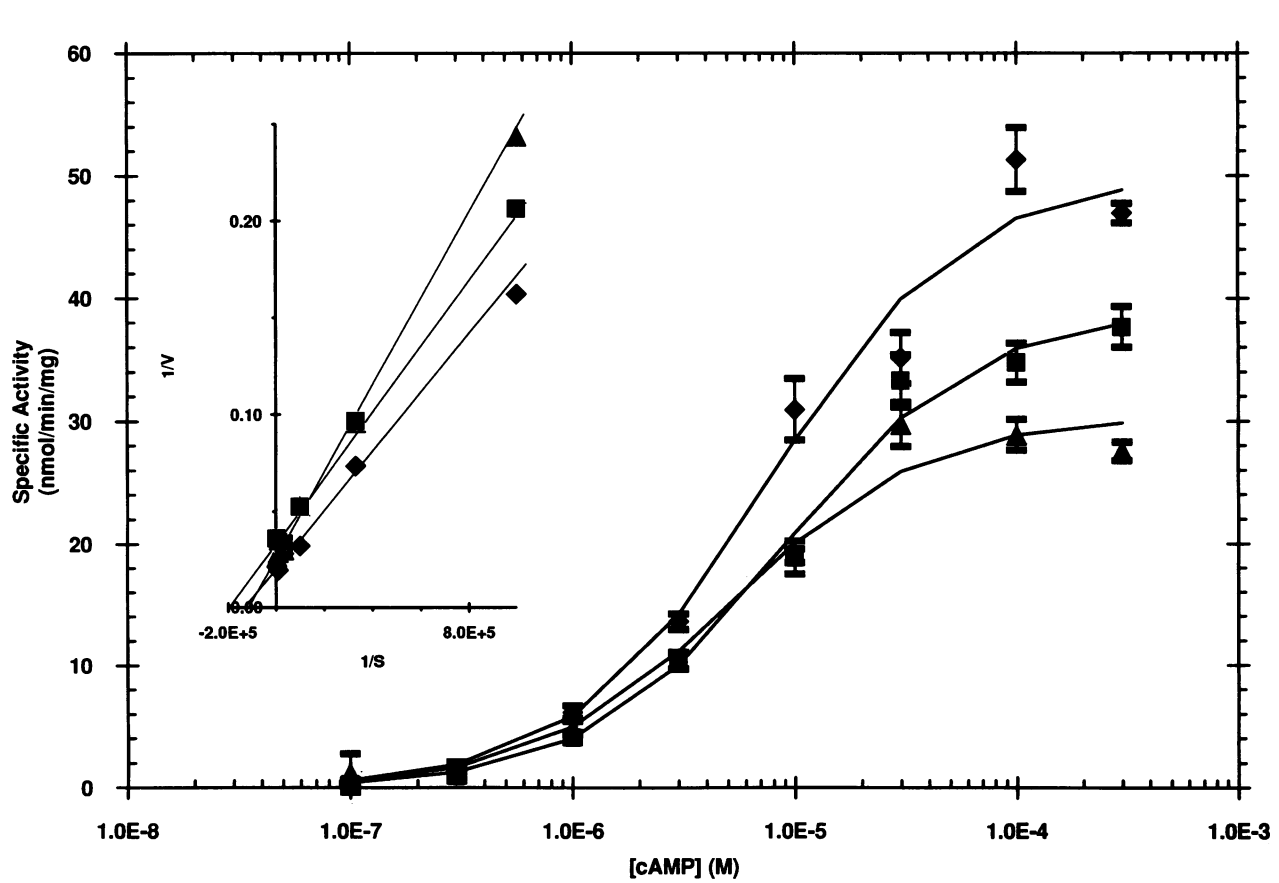

FIG. 6. Effect of cAMP concentration on the velocity of PDE activity associated with full-length cDNA clones for pTM72 (A) and *dnc* (B). Three separate pellets, derived from yeast cells harboring the respective plasmids, were lysed, and extracts were prepared as described in Materials and Methods. Hydrolytic rates as a function of the amount of enzyme were determined for eight substrate concentrations ranging from 1×10^{-7} to 3×10^{-4} M. The main graphs in both panels show specific activity as a function of cAMP concentration. The smooth curve describes the fit of a Michaelis-Menten model through the datum points. The error bars represent the standard error of the slope of the line fitted to the datum points determining the initial rates. (See Materials and Methods for details of data analysis.) The inset in each panel shows a Lineweaver-Burk transformation of the velocity data corresponding to substrate concentrations from 1×10^{-6} to 3×10^{-4} M. The lowest two concentrations of substrate were excluded from the plot to expand the axes.

human dunce-like PDEs displayed a pattern of potency expected for a cAMP-specific PDE. All were inhibited by IBMX, a nonspecific cyclic nucleotide PDE inhibitor, with no detectable difference in the concentration needed to produce 50% inhibition (IC_{50}). Inhibitors specific to other classes of PDEs, such as milrinone or cilostamide (inhibitors of cGMP-inhibited PDEs), 8-methoxy IBMX (an inhibitor of calcium-calmodulin-dependent PDEs), or zaprinast (an inhibitor of cGMP-specific PDEs), produced some inhibition, but at IC_{50}s 10- to 1,000-fold higher than those for their specific PDE classes (1, 27). All three human clones were markedly inhibited by the antidepressant drug rolipram, an inhibitor of the cAMP-specific PDEs, with IC_{50}s of 0.2 to 0.5 μM. The human *dnc* homologs were also inhibited by denbufylline (Table 3), an additional specific inhibitor of cAMP-specific PDEs. Dose-response curves for rolipram (Fig. 7B) and denbufylline inhibition of the human clones showed a relatively flat dose-response curve, which spread over 3 log units of inhibitor concentration. This property is consistent with the complex inhibitory kinetics previously reported for the human *dnc* homologs cloned by other groups (17, 24, 38).

The three human clones shared similar biochemical and pharmacologic properties. We were unable to detect more than a sixfold difference in the K_m for cAMP, and less than a threefold difference in the IC_{50} for denbufylline or roli-

TABLE 2. Summary of kinetic analysis for dunce PDE clones[a]

Locus	Plasmid	K_m (SD) in μM	Sp act (nmol/min/mg)
DPDE2[b]	pADH46R	18 (5.9)	21–64
DPDE3[b]	pADH43	8 (2.2)	54–138
DPDE4[b]	pADH72	7.2 (2)	29–50
dnc[b]	pADDROSF	27 (16)	0.8–5.6
dnc	pADDROSC	32 (9.5)	0.6–2.5

[a] Kinetic parameters were obtained for the hydrolysis of [^{3}H] cAMP (0.1 to 300 μM) from supernatants of yeast extracts derived from cells harboring the indicated plasmids. Values were determined in duplicate from three separate cell pellets. Each value for the K_m represents the average of six determinations, with the standard deviation shown in parentheses. The specific activity at V_{max} is reported as the range of determinations for the six experiments. All parameters were estimated with a Michaelis-Menten model as described in Materials and Methods.

[b] cDNAs truncated at amino-terminal end, as described in Results.

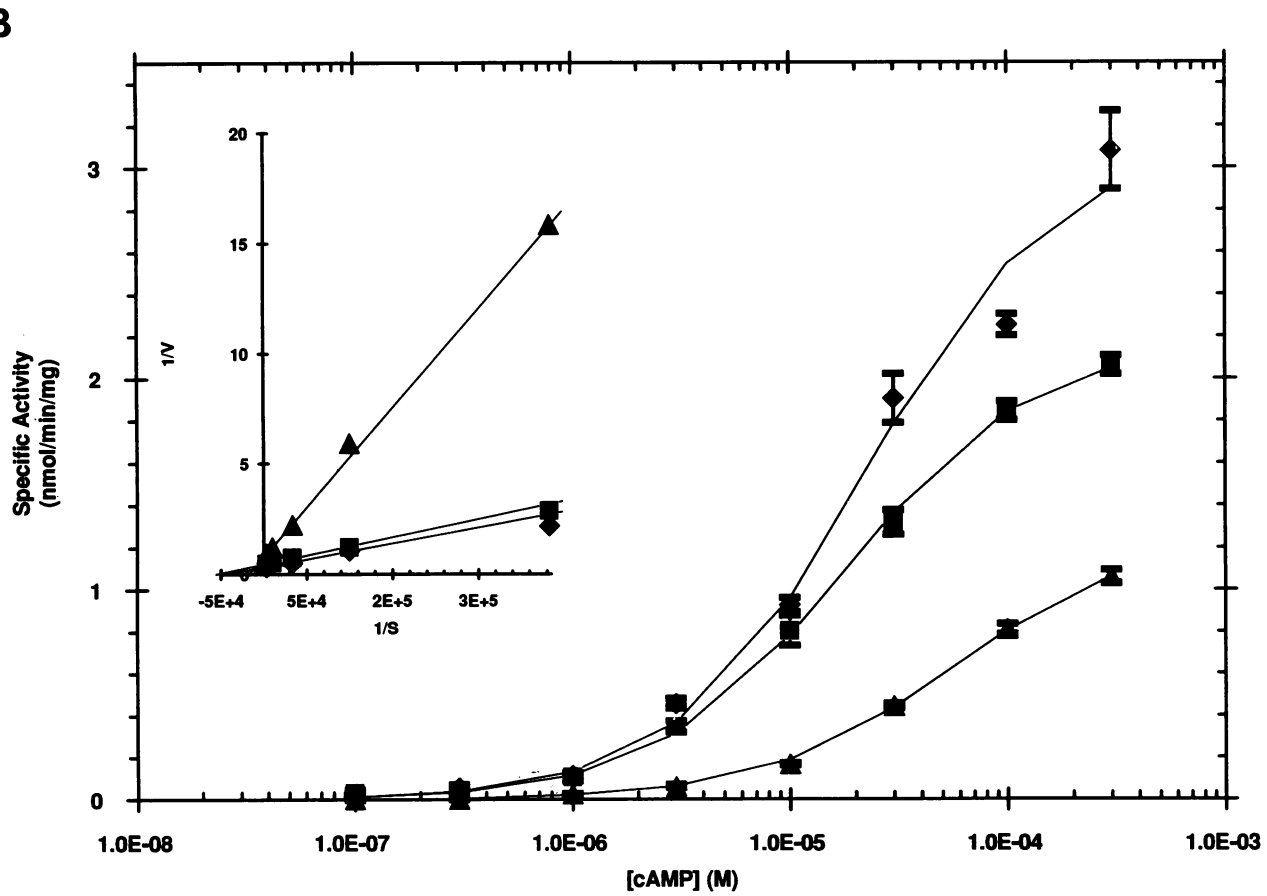

FIG. 6—*Continued.*

pram, among these clones (Table 3). For some of the cAMP-specific inhibitors, the pharmacologic properties of the human clones differed from those of *dnc*. The *dnc* gene product was not inhibited by rolipram or by Ro 20-1724 (IC_{50}s of >1,000 μM). Denbufylline exhibited substantial inhibitory activity for the *Drosophila dnc* clones (IC_{50} = 1 to 3 μM), although this activity is still approximately 10-fold lower than that for the human enzymes. Thus, the human and *Drosophila* cAMP-specific PDEs share many characteristics yet can be distinguished by specific inhibitors.

DISCUSSION

We have isolated cDNAs from four human loci with extensive homology to the *dnc* memory and learning gene of *D. melanogaster*. PCR analysis strongly suggested that these loci are the only ones encoding close homologs of *dnc* in the human genome. Biochemical and pharmacologic analysis of proteins encoded by cDNAs from three of the four human genes showed them to be cAMP-specific PDEs which were inhibited by the antidepressant drug rolipram. Northern blotting and RNase protection studies suggested that each of the genes has a distinctive pattern of cellular expression. The close homology of the human genes to *dnc*, their expression in the brain and in other tissues, and the inhibition of their encoded proteins by a drug with psychoactive properties suggests that they have an important functional role.

The human and *Drosophila dunce* genes share significant structural features with other cyclic nucleotide PDEs. However, the degree of homology among the *dunce* genes is much higher than that with any other PDE. Mammalian PDEs are divided into subgroups according to their biochemical and pharmacologic properties: I, Ca^{2+}-calmodulin-dependent PDEs; II, cGMP-stimulated PDEs; III, cGMP-inhibited PDEs; IV, cAMP-specific PDEs, which include the dunce PDEs; V, cGMP-specific PDEs; VI, photoreceptor PDEs; and VII, high-affinity, cAMP-specific PDEs (1, 25). All the vertebrate and insect PDEs that have been isolated to date contain a putative catalytic domain, located in the carboxyl one-third of the protein, with approximately 28 to 34% amino acid identity (1, 7, 9, 17, 25, 36). Evidence that this region contains the catalytic regions of the dunce PDEs has been shown by mutagenesis studies (15). The catalytic domains of members of any one PDE class are more strongly related than those of any two different classes, with, typically, 60 to greater than 90% homology. Outside the catalytic region, there is no region of sequence common to all PDE classes. However, the members of each class often share additional sequence motifs. These motifs are located in the amino termini of the protein and are generally postulated to have regulatory functions (1). For example, the type I PDEs are regulated, at least in part, by a presumptive calmodulin-interaction domain near their amino termini, and the type II PDEs are regulated by a cGMP-binding domain in the amino-terminal region of the protein. The interaction of the type VI PDEs with the G-protein transducin is also felt to occur in their amino-terminal regions (4, 35).

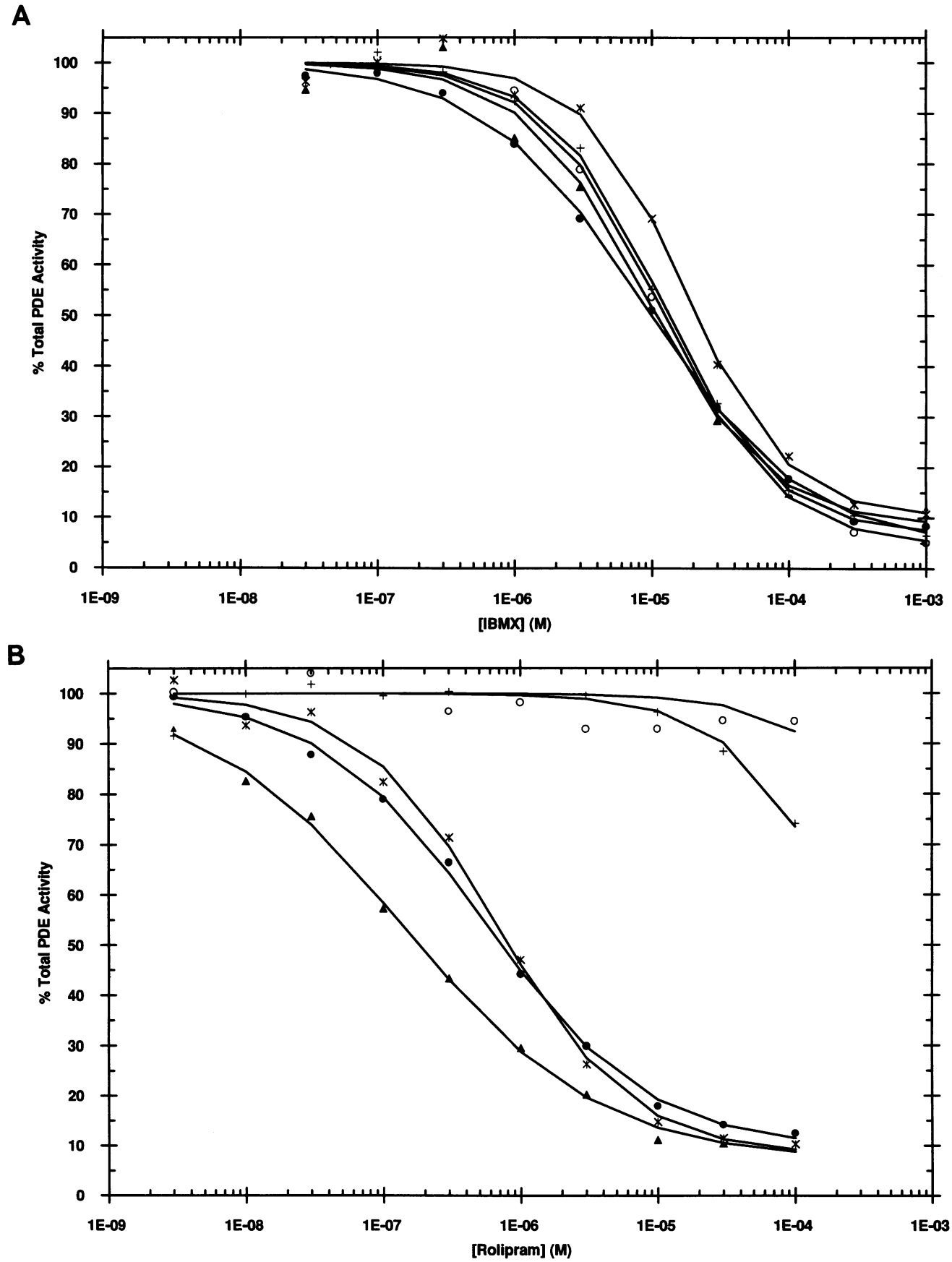

FIG. 7. Effect of IBMX (A) or rolipram (B) on enzyme activity of extracts from yeast cells harboring the following plasmids, as described in Table 3: pADDROSC (open circles), pADDROSF (crosses), pADH72 (asterisks), pADH46R (closed circles), and pADH43 (triangles). Dose-response inhibitory curves were calculated as described in Materials and Methods.

Our data show that *dnc* and its human homologs also contain a class-specific amino-terminal sequence motif. This motif is present in the 5′ region of our clones, a region absent, at least in part, from the rat or human *dnc* homologs reported previously (5, 7, 9, 17, 24, 36–38). The *D. melanogaster dnc* sequence, as most recently reported, is strongly homologous to this region of the human *dunce*-like genes (28). We have also shown (2) that the homology of the rat *dunce*-like genes extends further at the amino terminus than previously reported (5, 7, 9, 36–38). These amino-terminal regions contain two blocks of strong sequence homology, which we call UCR1 and UCR2, for upstream conserved regions (Fig. 1 and 2). UCR1 and UCR2 of humans and *D. melanogaster*, respectively, show more homology to each other than to any other sequences in the GenBank or EMBL data bases. UCR1 and UCR2 appear to be distinct, in that they lack homology to each other and are separated by a region of relatively low homology. Additionally, UCR1, but not UCR2, probably undergoes alternative splicing (e.g., in the pPDE32 clone [Fig. 1 and 2B]). Although the function of these regions is not known, sequence motifs that are strongly conserved in evolution are often functionally important. We speculate that UCR1 and UCR2, like the amino-terminal sequence motifs of other PDE classes, may have regulatory functions. One possibility is that UCR1 and/or UCR2 bind to other cellular proteins or cofactors. We are currently testing these hypotheses.

Our biochemical and pharmacologic analysis of human and *Drosophila dunce* clones demonstrates both similarities and differences between the proteins encoded by these genes. The *Drosophila* and human proteins have a similar K_m for cAMP but differ from 10- to several hundredfold in their IC_{50}s for mammalian cAMP-specific PDE inhibitors. Our data also show that the biochemical and pharmacologic properties of our three human clones are very similar. The physical basis for these differences and similarities is not clear. One possibility is the structure of the catalytic sites of these proteins. Alternatively, other aspects of the proteins, such as secondary modifications, resistance to proteolysis, or other properties, may explain our data. Although we were unable to obtain a full-length clone from the DPDE1 locus for testing in these assays, we expect that the biochemical properties of such a clone would be highly similar to those of the other human DPDE genes.

Our biochemical and pharmacologic data can be compared with those previously published by other groups. Two studies of the proteins encoded by human *dunce* cDNA clones expressed in mammalian cells or in *S. cerevisiae* have been published. Torphy et al. reported a K_m for the enzyme hPDE IV (which corresponds to a truncated version of the pPDE46/DPDE2 protein that we have analyzed) that is sixfold less than the K_m we report for pPDE46 (17, 39). McLaughlin et al. (24) reported a K_m for hPDE IVb, which corresponds to the splice variant of DPDE2 encoded by our pPDE32 clone, that is threefold less than the one we measured for this protein (21). Our data can also be compared with those of mammalian type IV enzymes extracted from natural sources (see Results and reference 7). The differences between these data and our results could reflect numerous factors. The results obtained for enzyme preparations derived from tissues or cells could reflect the contribution of several different PDE isozymes, as some of the reported preparations may not have been purified to homogeneity. Partial proteolysis (23) or other modifications could have occurred during the extraction or assay of our proteins. A potential limitation of our expression system is that yeast

TABLE 3. IC_{50}s for inhibition of dunce PDE clones[a]

Locus name	Plasmid	IC_{50} (μM) of inhibitor:								
		cAMP	cGMP	Denbufylline	Rolipram	IBMX	8-Methoxy IBMX	Milrinone	Cilostamide	Zaprinast
DPDE2[b]	pADH46R	9.7 (2.8)	>1,000[c]	0.22 (0.15)	0.5 (0.3)	9.3 (0.7)	220 (48)	59 (9)	140[c]	120 (38)
DPDE4[b]	pADH72	10 (1)	>1,000[c]	0.2 (0.2)	0.4 (0.02)	15 (4)	220 (7)	59 (70)	55 (13)	90 (8)
DPDE4	pADH72C	8.5 (0.9)	>1,000[c]	0.19 (0.03)	0.3 (0.01)	11 (2)	190 (74)	23 (2)	ND[d]	ND[d]
DPDE3[b]	pADH43	8.2 (1)	>1,000[c]	0.1 (0.01)	0.18 (0.04)	10 (2)	160 (13)	16 (7)	90[c]	88 (20)
dnc[b]	pADDROSF	54 (12)	>1,000[c]	1.5 (1.7)	>1,000[c]	11 (0.4)	120 (69)	>1,000[c]	>1,000[c]	130 (20)
dnc	pADDROSC	73 (63)	>1,000[c]	3 (0.5)	>740[c]	12 (0.3)	170 (17)	>1,000[c]	>1,000[c]	58 (2)

[a] IC_{50}s were obtained for the hydrolysis of 1 μM [^{3}H] cAMP from yeast extracts derived from cells harboring the indicated plasmids. The IC_{50} was determined by fitting the data to either a four-parameter model or a two-parameter model, as described in Materials and Methods. Wherever possible, the four-parameter model was used, because it could provide an accurate fit to inhibitor curves that spanned a wide range of concentrations. Data sets that could not be fitted to the four-parameter model were fitted to the two-parameter model. Each value represents the mean from two to five experiments. The values in parentheses represent the standard deviation of the mean for each experiment.

[b] cDNA truncated at the 5′ end, as described in Results.

[c] Data sets analyzed with the two-parameter model.

[d] ND, not determined.

cells may lack cellular functions needed for appropriate folding or secondary modification of the PDEs, or cofactors needed for physiologically complete enzyme function. The constructs may also be expressed at different levels, which may explain, for example, the lower specific activities we have obtained for the *Drosophila* clones, compared with the human ones (Table 2). Variations in assay methodology may account for some of the discrepancies: for example, many of the studies previously reported did not include substrate concentrations greater than 100 μM, and some did not exceed 30 μM. Finally, our recombinant proteins are designed to contain the first 13 amino acids from *S. cerevisiae* alcohol dehydrogenase fused to the amino terminus of the PDE, which may alter its kinetic properties.

Several lines of evidence suggest, but do not prove, that the mammalian dunce-like PDEs are the major in vivo targets for rolipram and other type IV PDE inhibitors. Biochemical and pharmacologic studies to date have failed to isolate any other enzymes that are inhibited as strongly by these drugs as are the type IV enzymes (1, 27). Binding studies have shown that the K_d of rolipram (approximately 1 nM) for cloned human dunce-like PDEs is similar to the concentration needed for therapeutic action in vivo (24, 39). Interestingly, this value is approximately 1,000-fold lower than that needed for enzyme inhibition. The reason for this discrepancy is unclear, but it may be related to the flattened inhibition curves that we and others have observed for many of the type IV-specific inhibitory compounds such as rolipram (see above and references 17, 24, and 39). The binding and inhibitory data both strongly support the use of cloned human *dunce*-like genes, expressed in *S. cerevisiae*, in assays for specific dunce PDE inhibitors (17, 24, 39).

The functions of the human dunce-like PDEs in the cell, or in the intact organism, remain open to speculation. It is also unclear whether these functions might differ among the four genes or among the different PDE isoforms produced by any one locus. The *dnc* locus was first isolated as a mutation affecting learning and memory in *D.* melanogaster (10), and cAMP pathways are important in learning in other organisms, notably *Aplysia* snails (33). The antidepressant effect of rolipram and other type IV PDE inhibitors suggests that the *dunce* genes also play an important function in the human CNS. However, dunce PDEs are expressed widely in tissues outside the CNS, and type IV PDE inhibitors may have other actions, including anti-inflammatory or immunomodulatory properties (1, 27, 39). Genetic approaches may be a powerful method of analyzing the functions of the mammalian *dnc* homologs. We and our collaborators (26) have determined the genetic mapping of the human and murine *dnc* homologs. Mapping the position of these loci may reveal an association of one of the genes with a previously described mutation. Study of such a mutation in turn may provide insight into the functions of the gene.

ACKNOWLEDGMENTS

We thank J. Wells for providing 8-methoxy IBMX; P. Feldman for providing zaprinast; N. Schaul, R. Decker, and H. Kloss for providing tissue specimens; and Y. Qiu and R. Davis for providing a *dnc* cDNA clone. We also thank K. McCaw, J. Meyer, G. Rosman, and S. Kalbfleisch for superb technical assistance; K. Loughney for manuscript review; C. Nicolette for assistance with the MACAW program; and P. Bird for typing the manuscript.

This work was supported by the National Cancer Institute and the American Cancer Society. M. Wigler is an American Cancer Society Research Professor.

REFERENCES

1. **Beavo, J. A., and D. H. Reifsnyder.** 1990. Primary sequence of cyclic nucleotide phosphodiesterase isozymes and the design of selective inhibitors. Trends Pharm. Sci. **11:**150–155.
2. **Bolger, G., L. Rodgers, M. Riggs, and M. Wigler.** Unpublished data.
3. **Bradford, M. M.** 1976. A rapid and sensitive method for the quantitation of microgram quantities of protein utilizing the principle of protein-dye binding. Anal. Biochem. **72:**248–254.
4. **Chabre, M., and P. Deterre.** 1989. Molecular mechanism of visual transduction. Eur. J. Biochem. **179:**255–266.
5. **Colicelli, J., C. Birchmeier, T. Michaeli, K. O'Neill, M. Riggs, and M. Wigler.** 1989. Isolation and characterization of a mammalian gene encoding a high-affinity cAMP phosphodiesterase. Proc. Natl. Acad. Sci. USA **86:**3599–3603.
6. **Colicelli, J., C. Nicolette, C. Birchmeier, L. Rodgers, M. Riggs, and M. Wigler.** 1991. Expression of three mammalian cDNAs that interfere with RAS function in *Saccharomyces cerevisiae*. Proc. Natl. Acad. Sci. USA **88:**2913–2917.
7. **Conti, M., and J. V. Swinnen.** 1990. Structure and function of the rolipram-sensitive, low-K_m cyclic AMP phosphodiesterases: a family of highly related enzymes, p. 243–266. *In* J. Beavo and M. D. Houslay (ed.), Cyclic nucleotide phosphodiesterases: structure, regulation and drug action. John Wiley and Sons Ltd., Chichester, West Sussex, England.
8. **Davis, R. L., and J. A. Kiger.** 1980. A partial characterization of the cyclic nucleotide phosphodiesterases of *Drosophila melanogaster*. Arch. Biochem. Biophys. **203:**412–421.
9. **Davis, R. L., H. Takayasu, M. Eberwine, and J. Myres.** 1989. Cloning and characterization of mammalian homologs of the *Drosophila* dunce$^+$ gene. Proc. Natl. Acad. Sci. USA **86:**3604–3608.
10. **Dudai, Y.** 1988. Neurogenetic dissection of learning and short-term memory in *Drosophila*. Annu. Rev. Neurosci. **11:**537–563.
11. **Eckmann, F., K. Fichte, U. Meya, and M. Sastre-Y-Hernandez.** 1988. Rolipram in major depression: results of a double-blind comparative study with amitriptyline. Curr. Ther. Res. **43:**291–295.
12. **Feng, D.-F., and R. F. Doolittle.** 1987. Progressive sequence alignment as a prerequisite to correct phylogenetic trees. J. Mol. Evol. **25:**351–360.
13. **Goldner, H., G. Dietz, E. Carstens, and J. Liebigs.** 1966. Synthesis of dibutylxanthine: "Eine neue Xanthin-Synthese." Ann. Chem. **691:**142–158.
14. **Henkel-Tiggs, J., and R. L. Davis.** 1990. Rat homologs of the *Drosophila dunce* gene code for cyclic AMP phosphodiesterases sensitive to rolipram and RO-20-1724. Mol. Pharmacol. **37:**7–10.
15. **Jin, S.-L. C., J. V. Swinnen, and M. Conti.** 1992. Characterization of the structure of a low K_m, rolipram-sensitive cAMP phosphodiesterase: mapping of the catalytic domain. J. Biol. Chem. **267:**18929–18939.
16. **Levin, L. R., P.-L. Han, P. M. Hwang, P. G. Feinstein, R. L. Davis, and R. R. Reed.** 1992. The *Drosophila* learning and memory gene *rutabaga* encodes a Ca^{2+}/calmodulin-responsive adenylyl cyclase. Cell **68:**479–489.
17. **Livi, G. P., P. Kmetz, M. M. McHale, L. B. Cieslinski, G. M. Sathe, D. P. Taylor, R. L. Davis, T. J. Torphy, and J. M. Balcarek.** 1990. Cloning and expression of cDNA for a human low-K_m, rolipram-sensitive cyclic AMP phosphodiesterase. Mol. Cell. Biol. **10:**2678–2686.
18. **Lugnier, C., M. Bruch, J.-C. Stoclet, M.-P. Strub, M. Marivet, and C. G. Wermuth.** 1985. Substituted carbostyrils as inhibitors of cyclic AMP phosphodiesterase. Eur. J. Med. Chem.-Chim. Ther. **20:**121–125.
19. **Lundberg, K. S., D. D. Shoemaker, M. W. W. Adams, J. M. Short, J. A. Sorge, and E. J. Mathur.** 1991. High-fidelity amplification using a thermostable DNA polymerase isolated from *Pyrococcus furiosus*. Gene **108:**1–6.
20. **MacDonald, R. J., G. H. Swift, A. E. Przybyla, and J. M. Chirgwin.** 1987. Isolation of RNA using guanidinium salts. Methods Enzymol. **152:**219–227.
21. **Martins, T. J., and K. M. Ferguson.** Unpublished data.

22. **Martins, T. J., M. C. Mumby, and J. A. Beavo.** 1982. Purification and characterization of a cGMP-stimulated cyclic nucleotide phosphodiesterase from bovine tissues. J. Biol. Chem. **255:**1973–1979.
23. **McHale, M. M., L. B. Cielinski, W.-K. Eng, R. K. Johnson, T. J. Torphy, and G. P. Livi.** 1991. Expression of human recombinant cAMP phosphodiesterase isozyme IV reverses growth arrest phenotypes in phosphodiesterase-deficient yeast. Mol. Pharmacol. **39:**109–113.
24. **McLaughlin, M. M., L. B. Cieslinski, M. Burman, T. J. Torphy, and G. P. Livi.** 1993. A low K_m, rolipram-sensitive, cAMP-specific phosphodiesterase from human brain: cloning and expression of cDNA, biochemical characterization of recombinant protein, and tissue distribution of mRNA. J. Biol. Chem. **268:**6470–6476.
25. **Michaeli, T., T. J. Bloom, T. Martins, K. Loughney, K. Ferguson, M. Riggs, L. Rodgers, J. A. Beavo, and M. Wigler.** 1993. Isolation and characterization of a previously undetected human cAMP phosphodiesterase by complementation of cAMP phosphodiesterase-deficient *Saccharomyces cerevisiae*. J. Biol. Chem. **268:**12925–12932.
26. **Milatovich, A., G. Bolger, M. Wigler, and U. Francke.** Unpublished data.
27. **Nicholson, C. D., R. A. J. Challiss, and M. Shahid.** 1991. Differential modulation of tissue function and therapeutic potential of selective inhibitors of cyclic nucleotide phosphodiesterase isoenzymes. Trends Pharm. Sci. **12:**19–27.
28. **Qiu, Y., C.-N. Chen, T. Malone, L. Richter, S. K. Beckendorf, and R. L. Davis.** 1991. Characterization of the memory gene dunce of *Drosophila melanogaster*. J. Mol. Biol. **222:**553–565.
29. **Rose, M. D., F. Winston, and P. Hieter.** 1990. Methods in yeast genetics: a laboratory course manual. Cold Spring Harbor Laboratory Press, Cold Spring Harbor, N.Y.
30. **Saiki, R. K., D. H. Gelfand, S. Stoffel, S. J. Scharf, R. Higuchi, G. T. Horn, K. B. Mullis, and H. A. Erlich.** 1988. Primer-directed enzymatic amplification of DNA with a thermostable DNA polymerase. Science **239:**487–491.
31. **Sambrook, J., E. F. Fritsch, and T. Maniatis.** 1989. Molecular cloning: a laboratory manual, 2nd ed. Cold Spring Harbor Laboratory Press, Cold Spring Harbor, N.Y.
32. **Schacher, S., D. Glanzman, A. Barzilai, P. Dash, S. G. N. Grant, F. Keller, M. Mayford, and E. R. Kandel.** 1990. Long-term facilitation in *Aplysia*: persistent phosphorylation and structural changes. Cold Spring Harbor Symp. Quant. Biol. **55:**187–202.
33. **Schuler, G. D., S. F. Altschul, and D. J. Lipman.** 1991. A workbench for multiple alignment construction and analysis. Proteins Struct. Funct. Genet. **9:**180–90.
34. **Short, J. M., J. M. Fernandez, J. A. Sorge, and W. D. Huse.** 1988. λZAP: a bacteriophage λ expression vector with *in vivo* excision properties. Nucleic Acids Res. **16:**7583–7600.
35. **Stryer, L.** 1986. Cyclic GMP cascade of vision. Annu. Rev. Neurosci. **9:**87–119.
36. **Swinnen, J. V., D. R. Joseph, and M. Conti.** 1989. Molecular cloning of rat homologues of the *Drosophila melanogaster* dunce cAMP phosphodiesterase: evidence for a family of genes. Proc. Natl. Acad. Sci. USA **86:**5325–5329.
37. **Swinnen, J. V., D. R. Joseph, and M. Conti.** 1989. The mRNA encoding a high-affinity cAMP phosphodiesterase is regulated by hormones and cAMP. Proc. Natl. Acad. Sci. USA **86:**8197–8201.
38. **Swinnen, J. V., K. E. Tsikalas, and M. Conti.** 1991. Properties and hormonal regulation of two structurally related cAMP phosphodiesterases from the rat Sertoli cell. J. Biol. Chem. **266:**18370–18377.
39. **Torphy, T. J., J. M. Stadel, M. Burman, L. B. Cieslinski, M. M. McLaughlin, J. R. White, and G. P. Livi.** 1992. Coexpression of human cAMP-specific phosphodiesterase activity and high affinity rolipram binding in yeast. J. Biol. Chem. **267:**1798–1804.
40. **Zhong, Y., and C.-F. Wu.** 1991. Altered synaptic plasticity in *Drosophila* memory mutants with a defective cyclic AMP cascade. Science **251:**198–201.